

## Parameter Identification of Actuator Nonlinear Model based on Limit-Cycle Phenomenon

**Bueno, A. M.**

Instituto Nacional de Pesquisas Espaciais – INPE.  
 Av. dos Astronautas, 1758 – São José dos Campos – SP  
[atila.bueno@uol.com.br](mailto:atila.bueno@uol.com.br)

**Leite Filho, W. C.**

Instituto de Aeronáutica e Espaço – IAE.  
 Pça Marechal Eduardo Gomes, 50 – São José dos Campos - SP  
[waldemar@iae.cta.br](mailto:waldemar@iae.cta.br)

**Abstract.** *The attitude control of space vehicles is fundamental to accomplish a mission. This system faces several types of problems, among them stands out actuator's nonlinearities. The actuator's (movable nozzle) nonlinearities cause the limit-cycle phenomenon, which impairs the control system design. This work aims to determine the parameters of actuator which cause the limit-cycle phenomenon. In order to do that, it is presented a method of identification based on the first harmonic analysis and data obtained from hardware in the loop simulation. The describing function approach leads to analytical solution to obtain nonlinear parameters. Digital simulation using such results is compared to hardware in the loop tests.*

**Keywords.** *Actuators, nonlinear model, parameter identification, limit-cycle.*

### 1. Introduction

In the design of control systems, it is usual to face problems which solutions have to compromise two, or even more, design criteria. Such kind of problem happens regarding the attitude control system of space vehicles.

The vehicle flexibility effect must be attenuated, otherwise it will become unstable. This is usually done by a notch filter tuned at the bending frequency, but the notch filter also affects the limit-cycle. On the other hand, the limit-cycle is usually adjusted by a lead filter, which may lead to instability due to the bending modes.

The limit-cycle is caused by the actuator's nonlinearities. Since nonlinearities cannot be modified or even cancelled, it is necessary to have a strategy to modify the limit-cycle. The sensitivity of the limit-cycle frequency regarding the nonlinear parameter helps to find out such strategy.

To study this problem, the first step is to obtain a nonlinear model of the actuator. Although it is possible to find, by digital simulation, the values that reproduce the limit-cycle, it is not possible to be sure that they are the real values because the solution is not unique.

The first harmonic analysis yields describing functions which permit to find a set of equations defined by the conditions to the limit-cycle existence. The real data, obtained from the hardware in the loop simulation (frequency and amplitude of the limit-cycle), are used to solve the equations and to determine the nonlinear parameters values.

### 2. Model Structure

The model proposed (Ferreira, 1996) to the actuator (Fig. 1) contains a 2<sup>nd</sup> order transfer function  $G_A(S)$ , a gain  $K$  and an integrator. This constitutes the 3<sup>rd</sup> order linear part of the model. The transport delay at the output is considered well known and its value is 7 milliseconds (Silva, 1998).

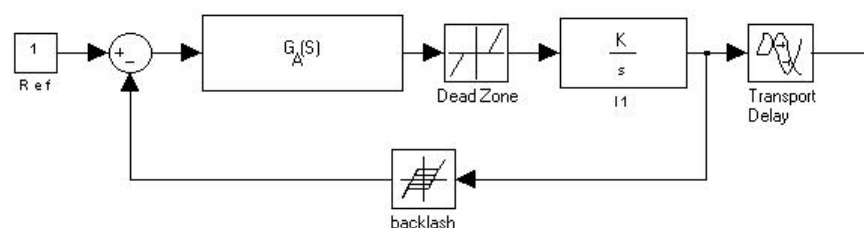


**Figure 1:** Proposed actuator model<sup>1</sup>

The linear part of the model,  $G_A(S)$  and the gain  $K$ , was determined by the ARX algorithm, using sampled data of the actuator's response to steps inputs. Thus,  $KG_A(S)$  is given by:

$$KG_A(s) = \frac{37 \cdot 34100}{s^2 + 370s + 34100} \quad (1)$$

The values of the nonlinear elements  $zm$  (dead-zone) and  $f$  (backlash), are determined by the solution of the set of equations, which define the conditions of limit-cycle existence.

### 3. Hardware in the loop simulation

The hardware in the loop simulation consists of a simplified model of the vehicle and a PD controller, both digitally implemented. The real actuator is also present and is activated by a D/A card. The displacement of the actuator is measured by a displacement sensor, which is connected to an A/D card. Fig. (2) shows the block diagram of the simulation. The sampling frequency (200 Hz) is high enough, so that the digitization effects can be neglected.

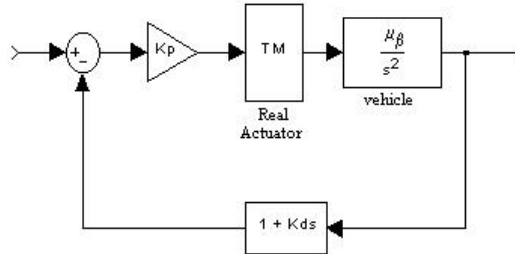


**Figure 2:** Hardware in the loop simulation

As an example, let's consider  $K_p=9.8$ ,  $K_d=0.06$  and  $\mu_\beta=4.5$ . Fig. (3) shows the response of both actuator and vehicle model. As it can be seen the limit-cycle phenomenon is present, and its frequency and amplitude can be measured. The gain and phase lag of the actuator are now available, and are used in the identification process.

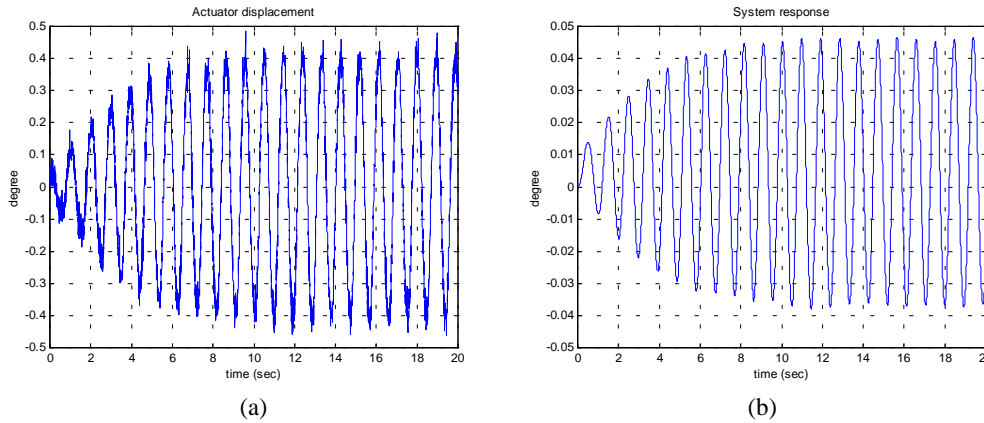


**Figure 3:** Actuators and system response

### 4. The First Harmonic Analysis.

The first harmonic analysis states that if a nonlinear element is been excited by a sinusoidal wave, and all Fourier Transform's components - except the fundamental - can be neglected, then the nonlinear element may be approximated by a describing function. Since the limit-cycle looks like a sinusoidal wave, as can be seen in the Fig. (4), the first harmonic analysis is indicated.

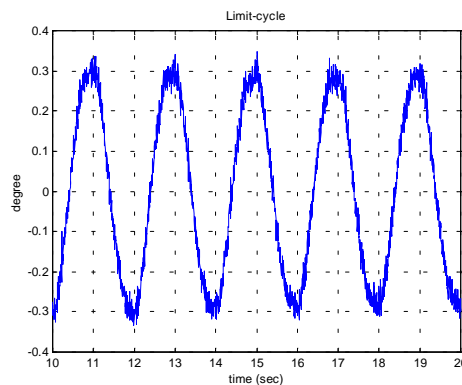


**Figure 4:** Limit-cycle from the Hardware in the loop simulation.

The describing function is defined as the complex ratio of the fundamental component of the nonlinear element by the input sinusoid (Slotine, 1991), i.e.:

$$N(X, \omega) = \frac{Y_1}{X} \angle \phi_1 \quad (2)$$

where  $Y_1$  and  $X$  are the amplitudes of the fundamental component and the input respectively,  $\phi_1$  is the phase of the fundamental component,  $\omega$  is the frequency of the input sinusoid.

Fig. (1) shows that there are two nonlinear elements in the model – dead-zone and backlash - which are approximated by its describing functions. The dead-zone describing function is given by:

$$Z(X_z) = \frac{2}{\pi} \left( \frac{\pi}{2} - \sin^{-1} \left( \frac{zm}{X_z} \right) - \frac{zm}{X_z} \sqrt{1 - \frac{zm^2}{X_z^2}} \right) \quad (3)$$

which is a real gain since the dead-zone is an odd function. The backlash's describing function is:

$$|F(X_f)| = \frac{1}{X_f} \sqrt{a_1^2 + b_1^2} \quad \text{and} \quad \angle F(X_f) = \tan^{-1} \left( \frac{a_1}{b_1} \right) \quad (4)$$

with the Fourier coefficients  $a_1$  and  $b_1$  given by:

$$a_1 = \frac{4f}{\pi} \left( \frac{f}{X_f} - 1 \right) \quad \text{and} \quad b_1 = \frac{X_f}{\pi} \left[ \frac{\pi}{2} - \sin^{-1} \left( \frac{2f}{X_f} - 1 \right) - \left( \frac{2f}{X_f} - 1 \right) \sqrt{1 - \left( \frac{2f}{X_f} - 1 \right)^2} \right] \quad (5)$$

and as can be seen, both  $Z(X_z)$  and  $F(X_f)$  do not depend on  $\omega$ .

The model of the actuator with the describing functions can be seen in Fig. (5).

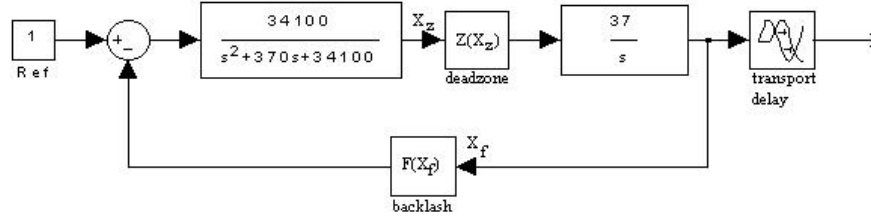


**Figure 5:** The actuator's model with describing functions.

The condition for the existence of limit-cycles (Gibson, 1963) in systems like the one shown in Fig. (6), is that:

$$G(j\omega) = -\frac{1}{N(X)} \quad (6)$$

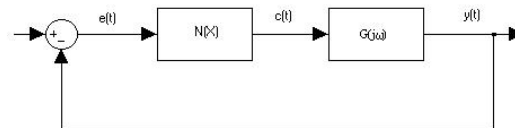


**Figure 6:** A nonlinear system block diagram

In other words,  $G(j\omega).N(X)$  should have the gain 1 and the phase lag equals to  $-180^\circ$ .

## 5. The method

In order to obtain the parameters that produce the limit-cycle phenomenon, the system in Fig. (2) is rearranged in Fig. (7). Then, it is possible to separate transfer functions of actuator and of plant.

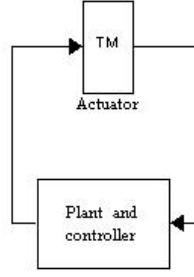


**Figure 7:** Block diagram expressing the actuator and vehicle plus controller dynamics

The transfer function of the plant plus controller is given by:

$$G_p(s) = \frac{K_p \mu_\beta (1 + K_d s)}{s^2} \quad (7)$$

thus:

$$|G_p(j\omega)| = \frac{K_p \mu_\beta}{\omega^2} \sqrt{1 + (K_d \omega)^2} \quad \text{and} \quad \phi_p = \tan^{-1}(k_d \omega) \quad (8)$$

The actuator's transfer function, considering the describing functions of the nonlinearities, is given by:

$$G_m(s, Z, F, T_d) = \frac{37 \cdot 34100 Z(X_z)}{s^3 + 370s^2 + 34100s + 37 \cdot 34100 Z(X_z) F(X_f)} e^{-T_d s} \quad (9)$$

where  $Z(X_z)$  and  $F(X_f)$  are given by equations (3) and (4) respectively, thus

$$|G_m(j\omega, Z(X_z), F(X_f), T_d)| = \frac{37 \cdot 34100 Z(X_z)}{\sqrt{\left( \frac{37 \cdot 34100 Z(X_z) R_f}{K_1} - 370\omega^2 \right)^2 + \left( 34100 \left( \frac{37 Z I_f}{K_1} + \omega \right) - \omega^3 \right)^2}} \quad (10)$$

where  $K_1 = X_f$  is the amplitude of the limit-cycle in the actuator output and  $\omega$  its frequency,  $F(X_f) = R_f + j \cdot I_f$  and

$$\phi_m = -\tan^{-1} \left( \frac{34100 \left( \frac{37 Z I_f}{K_1} + \omega \right) - \omega^3}{\frac{37 \cdot 34100 Z R_f}{K_1} - 370\omega^2} \right) - T_d \omega. \quad (11)$$

The first harmonic analysis indicates that when the Eq. (6) has a solution, the limit-cycle exists. Applying the Eq. (6) to the system described in the Fig.(7), it yields:

$$|G_m(j\omega, Z, F, T_d)| = \frac{1}{|G_p(j\omega)|} \quad \text{and} \quad \phi_m + \phi_p = -\pi \quad (12)$$

Let  $Z_x = 37 \cdot 34100 \cdot Z(X_z)$  and Eq. (11) squared yields:

$$\frac{Z_x^2}{\left( Z_x \frac{R_f}{K_1} - 370\omega^2 \right)^2 + \left( Z_x \frac{I_f}{K_1} + 34100\omega - \omega^3 \right)^2} = \frac{1}{|G_p(j\omega)|^2} \quad (13)$$

Substituting Eq. (11) on (12b), and after some manipulation, results:

$$Z_x \frac{R_f}{K_1} - 370\omega^2 = \frac{Z_x \frac{I_f}{K_1} + 34100\omega - \omega^3}{\tan(\pi + \phi_p - T_d\omega)} \quad (14)$$

Substituting Eq. (14) on (13) it results:

$$\frac{Z_x^2}{\left(Z_x \frac{I_f}{K_1} + 34100\omega - \omega^3\right)^2} = \left[ \frac{1 + \frac{1}{\tan(\pi + \phi_p - T_d\omega)}}{|G_p(j\omega)|} \right]^2 = KK \quad (15)$$

Since KK is a value determined by the hardware in the loop test (limit-cycle frequency  $\omega$  and its amplitude K1 besides the gain and phase of  $G_p(j\omega)$ ), it is possible to solve Eq. (15) for  $Z_x$ , which yields:

$$\left[ 1 - \left( \frac{I_f}{K_1} \right)^2 KK \right] Z_x^2 - 2(34100\omega - \omega^3) \frac{I_f}{K_1} KK Z_x - (34100\omega - \omega^3) \cdot KK = 0 \quad (16)$$

$$Z_x = \frac{(34100\omega - \omega^3) \left[ \frac{I_f}{K_1} KK + \sqrt{KK} \right]}{1 - \left( \frac{I_f}{K_1} \right)^2 KK} \quad (17)$$

$$\text{Considering Fig. (5) and the actuator output amplitude of limit-cycle } K_1 \text{ its possible to say that } X_z = \frac{K_1 \omega}{37 Z_x} \quad (18)$$

Eq. (17) gives the value of the dead-zone gain from an arbitrary backlash (Eq. 5). Thus, it is possible to obtain a set of possible solutions for the limit-cycle, but the real solution must satisfy Eq. (12). The dead-zone  $z_m$  can be calculated from Eqs. (3) and (18).

## 6. Results

The hardware in the loop simulation gives the frequency and the amplitude of the limit-cycle for a certain set of the controller gains. Let  $k_p = 5.84$ ,  $k_d = 0.062$  and  $\mu_\beta = 12.3$ , the amplitude and frequency obtained from the simulation are  $K_1 = 4.89 \times 10^{-3}$  rad and  $\omega = 8.57$  rad/s (Fig. 7).

The values of the parameters obtained with the presented method are  $f = 0.0004364$  rad (backlash) and  $z_m = 0.0012$  rad (dead-zone). The digital simulation (Fig. 8) yields the limit-cycle in the Fig. (9). As it can be seen in the Fig. (9) the amplitude of the limit-cycle is  $5.0 \times 10^{-3}$  rad and the frequency is 8.57 rad/s.

The digital simulation shows that the values of the parameters of the nonlinearities, obtained from the presented method, generates the limit-cycle and the frequency and amplitude fits very well. However, there is some discrepancy with the shape of the wave, which is not a perfect sinusoid. These problems are generated by the model, that shall be refined.

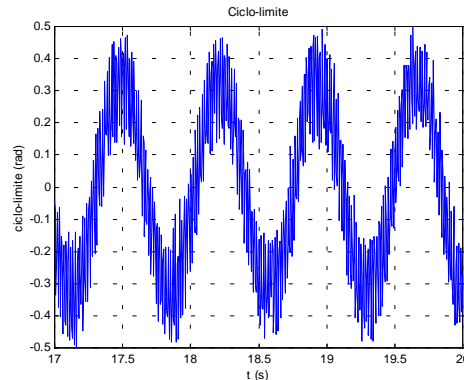


**Figure 7:** Limit-cycle from the hardware in the loop simulation

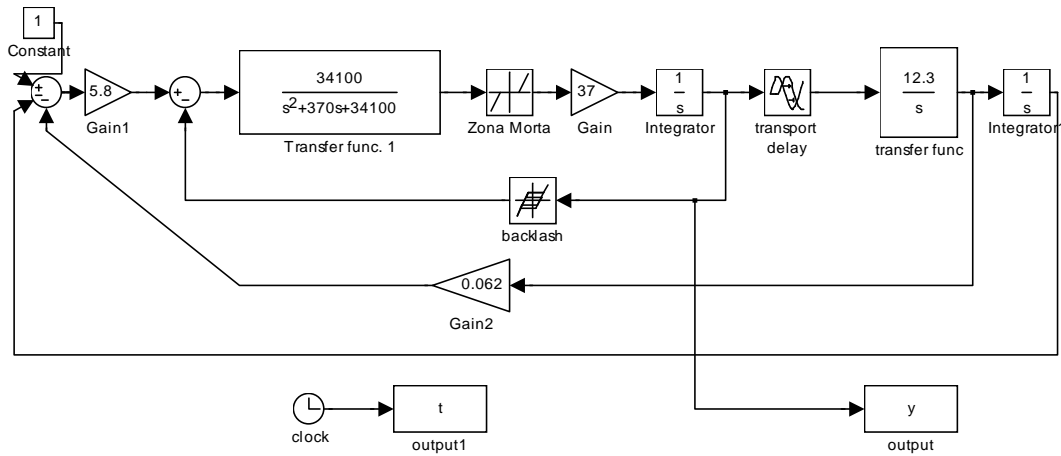


**Figure 8:** Digital simulation

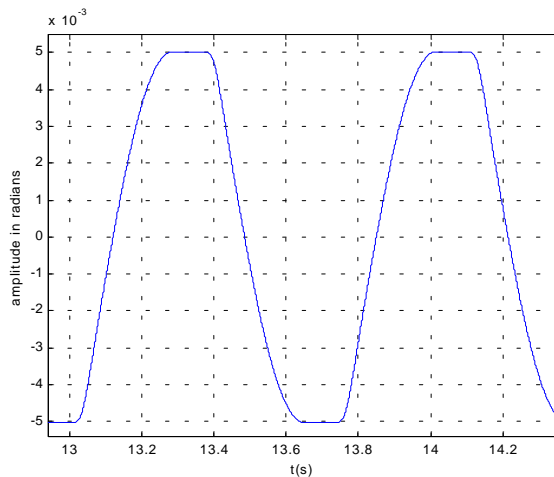


**Figure 9:** Limit-cycle from the digital simulation

## 7. Conclusion

This paper presents a method for the parameter identification of a nonlinear model, based on the first harmonic analysis and data obtained from the hardware in the loop simulation. The method is applicable in cases where the first harmonic analysis is indicated and the limit-cycle phenomenon exists.

Although there is some discrepancy in the shape, the limit-cycle obtained from the model has the same value of frequency and very close amplitude to that obtained from the hardware in the loop simulation. This discrepancy in the shape of wave indicates that the actuator model has to be improved.

The presented method gives an analytic solution for the parameters, which makes the computer program easier to implement. Although some algebraic manipulation is needed, the method is quite simple and efficient.

## 8. References

- Ferreira, S.B., 1996, **Análise do ciclo-limite devido à não-linearidade no atuador em malha de controle de atitude**, Instituto Tecnológico de Aeronáutica, CBU 629.7.036.5.
- Gibson, J. E., 1963, **Nonlinear Automatic Control**. Mcgraw-Hill.
- Silva, S., 1998, **Memorando Técnico sobre análise de dados para identificação da Tubeira Móvel**, IAE/ASE.
- Slotine, J-J E.; LI W; 1991, **Applied Nonlinear Control**, Prentice-Hall.